IBRACON Structures and Materials Journal
Revista IBRACON de Estruturas e Materiais
ISSN 1983-4195 ismj.org

ORIGINAL ARTICLE

Comparative analysis of multilinear constitutive models of steel fiber reinforced concrete

Análise comparativa de modelos constitutivos multilineares de concreto reforçado com fibras de aço

Flávia Fasolo[a]
Henrique Machado Kroetz[b]
Ricardo Pieralisi[c]

[a]Universidade Federal do Paraná – UFPR, Programa de Pós-graduação em Engenharia Civil – PPGEC, Curitiba, PR, Brasil
[b]Universidade Federal do Paraná – UFPR, Centro de Estudos do Mar, Pontal do Paraná, PR, Brasil
[c]Universidade Federal do Paraná – UFPR, Centro de Estudos de Engenharia Civil – CESEC, Programa de Pós-graduação em Engenharia Civil – PPGEC, Curitiba, PR, Brasil

Received 14 February 2023
Revised 01 June 2023
Accepted 15 June 2023
Corrected 27 March 2024

Abstract: The challenging task of structural design under structural safety, economic efficiency and environmental sustainability constraints has led to the development of several efficient materials. In this context, steel fiber reinforced concrete (SFRC) stands out due to the post-cracking behavior related to its enhanced toughness. Recent structural design normative codes consider this composite, suggesting good structural performance and broadening its applicability. Nevertheless, literature still lacks a comprehensive constitutive model to precisely describe its tensile behavior. This paper analyzes and compares three of the main European constitutive models, investigating factors that possibly influence their behavior. This study was conducted based on the cross-sectional analysis method, so that load-CMOD graphs could be obtained. Statistical analysis was conducted to classify the models, regarding several relevant parameters, such as mean compressive strength of the matrix and fiber volume. Results show that the constitutive law proposed by the fib Model Code shows the best performance. Also, from the set of considered parameters, ultimate tensile fibers strength presents the greatest sensitivity concerning structural post-crack behavior.

Keywords: fiber reinforced concrete, constitutive equations, sectional analysis, steel fiber.

Resumo: A desafiadora tarefa de projetar estruturas com segurança, eficiência econômica e sustentabilidade ambiental levou ao desenvolvimento de diversos materiais eficientes. Nesse contexto, cabe destacar o concreto reforçado com fibras de aço (CRFA), dado o seu comportamento pós-fissuração propiciado pela incorporação de fibras no concreto. Códigos normativos recentes de projeto estrutural abordam esse compósito, sugerindo um bom desempenho estrutural o que colabora para ampliar a sua aplicabilidade. Apesar disso, a literatura ainda carece de um modelo constitutivo abrangente para descrever com precisão seu comportamento à tração. Este artigo analisa e compara três dos principais modelos constitutivos europeus, investigando fatores que possivelmente influenciam seu comportamento. Este estudo foi conduzido com base no método de análise de seção transversal, para que os gráficos de carga-CMOD pudessem ser plotados. Uma análise estatística foi realizada para classificar os modelos em relação a alguns parâmetros relevantes, tais como a resistência à compressão média da matriz e o volume de fibras. Os resultados mostram que a lei constitutiva proposta pela fib Model Code apresenta o melhor desempenho. Além disso, do conjunto de parâmetros considerados, a resistência à tração das fibras apresenta a maior sensibilidade com relação ao comportamento estrutural de pós-fissuração.

Palavras-chave: concreto reforçado com fibras, equações constitutivas, análise de seção, fibras de aço.

How to cite: F. Fasolo, H. M. Kroetz, and R. Pieralisi, "Comparative analysis of multilinear constitutive models of steel fiber reinforced concrete," *Rev. IBRACON Estrut. Mater.*, vol. 17, no. 3, e17309, 2024, https://doi.org/10.1590/S1983-41952024000300009

Corresponding author: Flávia Fasolo. E-mail: flaviarfasolo@gmail.com
Financial support: This study was financed in part by the Coordenação de Aperfeiçoamento de Pessoal de Nível Superior – Brasil (CAPES) – Finance Code 001 and the research project CNPq/MCTI/FNDCT Nº 18/2021 422189/2021-9.
Conflict of interest: Nothing to declare.
Data Availability: The data that support the findings of this study are available from the corresponding author, [FF], upon reasonable request.
This document has an erratum: https://doi.org/10.1590/S1983-41952024000300011

1 INTRODUCTION

Traditionally, the reinforcement of concrete structures is carried out with continuous steel bars added at appropriate positions to support the imposed stresses. However, advances in research have proven that fibers can be used to partially or totally replace traditional reinforcement. Fiber Reinforcement Concrete (FRC) is thus a competitive alternative in structural design [1].

The incorporation of short and discontinuous fibers in the concrete mix plays an important role in improving its mechanical properties, especially to its post-cracking behavior. This type of three-dimensional reinforcement provides an enhanced crack-bridging capacity, increasing concrete toughness and durability, which can be very convenient for certain applications [2].

To extend the use of FRC as a structural solution, it is essential to have models that reliably reflect its behavior. However, given its complexity, the development of constitutive laws that allow an adequate characterization of the tensile behavior of this material is a challenge. The emergence of codes and guidelines that define the basis for calculating the FRC has been an important tool, since they give the designer greater security in the solutions adopted for this type of structure [3]. Nonetheless, after numerous proposals, there is no constitutive model broadly accepted, this is mainly due to differences proposed in each document [4].

However, it is important to highlight the significant progress made in the field of SFRC. An example is the recent publication of the Brazilian regulation NBR 16935 [5], which establishes the first design procedure for FRC structures in the country. Additionally, noteworthy updates in project codes have been observed in other countries as well. For instance, in Spain, the Codigo Estructrural [6] has replaced the previous Instrucción de Hormigon Estructural [7], and in Germany, the DAfStb-Richtlinie Stahlfaserbeton [8] has replaced the DBV-Merkblatt Stahlfaserbeton [9].

From this perspective, it is evident that the latest guidelines and codes compile previous experiences, leading in improvements in mechanical response, production methods, quality control, testing, and calculation methods. Despite these advancements, challenges still exist regarding the suitability of SFRC for certain applications. To address this situation, continuous studies and research are necessary to investigate means of predicting the behavior of this composite, taking into account potential influencing factors.These studies hold significance as the constitutive laws, despite sharing certain similarities such as the utilization of discontinuous equations and an indirect approach, exhibit differences in their format and parameter definition. These disparities can lead to variations in their predictions. Therefore, conducting a comparative study becomes essential to assess the capability of constitutive models in predicting the behavior of FRC elements [10].

Furthermore, there is a large variety of fibers and concretes commercially available. This allows a wide range of possibilities to design and manufacture FRC mixes. Such materials have properties that not only can significantly affect their mechanical performance, but also influence each other. Therefore, the study of the relationship of these factors with the prediction of behavior by the models also represents an important issue [11].

To conduct a comprehensive examination of the existing constitutive models and their associated parameters, it is crucial to perform numerical analysis. Two prominent approches in this regard are the diffuse cracking theory and the discrete cracking theory. In the diffuse crack theory, cracks are distributed throughout the continuous solid, while the discrete crack theory predefines crack locations and explicitly represents the fibers. The discrete crack theory offers a more accurate representation of the structural behavior of FRC, considering precise information on fiber volume and orientation. However, simulating discrete fibers may be challenging due to material nonlinearities and substantial computational time required [12], [13].

Additionally, employing constitutive equations to simulate the tension response of FRC structural elements may simplify numerical analysis. This involves determining the necessary parameters and assumptions to replicate the behavior of the element. Subsequently, a calculation algorithm, often based on the section analysis method, is employed to obtain the stress-strain response of the constituent materials. The numerical results can then be compared with experimental data, providing insight into the appropriateness of the constitutive equation and its defining parameters [4].

Considering these approaches, the discrete crack theory, with its consideration of crack locations and explicit fiber representation, offers a superior approximation of the structural behavior of FRC. However, its application requires specialized algorithms and significant computational resources. As a result, for civil engineering applications, the adoption of cross-sectional analysis is prevalent due to its lower computational cost. Many studies continue to employ this method while making necessary adjustments based on specific conditions.

Taking all this into account, this paper examines the analytical simulation of the flexural response of SFRC beam test using the main European models. For this purpose, a literature review was conducted to gather data from several three-point-bending tests of beams, standardized by EN 14651 [14], composed of different types of concrete and fibers. Data extracted from the literature were simulated using a model based on cross-sectional analysis.

These simulations made it possible to compare the responses of different European constitutive models. In addition, possible factors that influence the prediction of the bending behavior of SFRC by the constitutive laws were also

evaluated. This is intended to provide useful information to designers, which will allow them to select, in addition to the constitutive law, concrete and fiber characteristics that are more appropriate to satisfy the desired mechanical requirements for the SFRC in question.

2 DATA COLLECTION

2.1 Materials

A comprehensive database containing information on post-cracking strengths determined using three-point bending tests was considered [15]. This database is the result of 81 series of tests for a total of 528 SFRC beams. Additionally, two other references [13], [16] with three series of results each, were included to increase the amount of data and the representativeness of the results.

The data includes a wide variety of concretes, covering various ranges of compressive strength, volume fraction of fibers, fiber aspect ratio, and fiber tensile strength. An overview of the data collected is presented in Figure 1, regarding:

- Mean compressive strength, ranging between 30 and 90 MPa;
- Volume fraction of fibers, from 0.32% to 1%.
- Fiber length, ranging from 30 to 80 mm;
- Fiber diameter, ranging from 0.3 mm to 1.0 mm;
- Fiber aspect ratio, ranging from 44 to 100;
- Fiber tensile strength, ranging from 1100 to 3100 MPa.

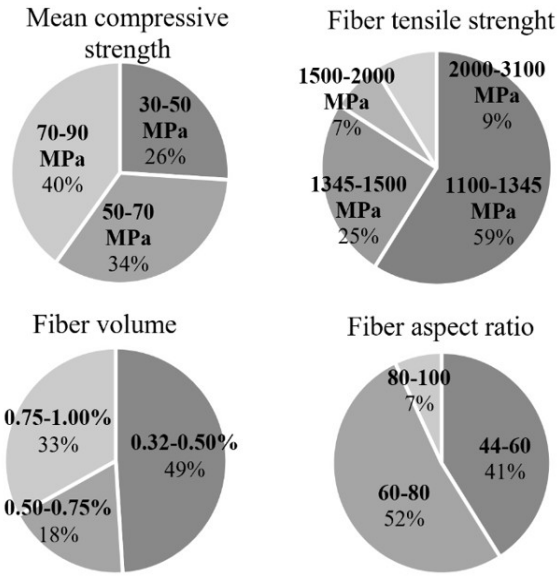

Figure 1. Distribution of properties of concrete and fibers.

It was analyzed, besides the main European constitutive models, the compressive strength of the concrete matrix, as well as the volume, the fiber aspect ratio, and the tensile strength of the fibers, given their possible influences on the residual strength of FRC.

2.2 Test setup and specimens

The experimental test results, as documented in the literature and conducted by the aforementioned authors, were performed using a three-point bending configuration following the guidelines of EN 146517 [14]. In general, prismatic beams with spans of 450 mm and 500 mm, total lengths of 500 mm and 550 mm, respectively, cross section of 150 x 150 mm, and a 25 mm deep notch located at mid-span of the beam were used. Figure 2 illustrates an example of the main configuration employed. Within this test method, two control configurations can be adopted: eiher by measuring the notch opening (CMOD) or by measuring the vertical displacement of the specimen (δ). For the purposes of this study, the control configuration based on CMOD was selected for the comparison.

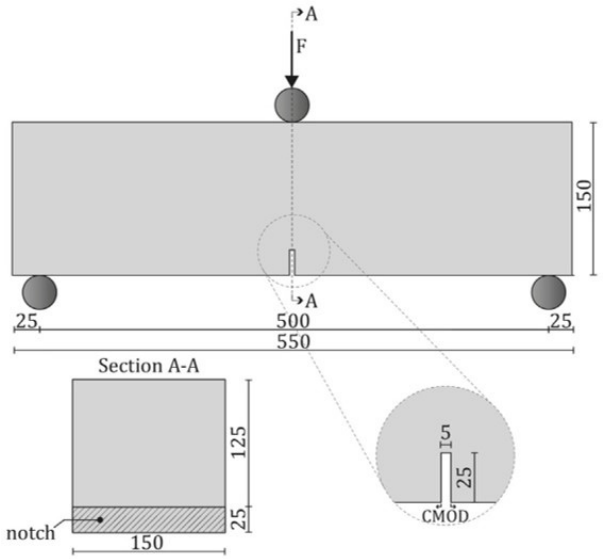

Figure 2. Specimen geometry of the three-point bending test according to EN 14651 [14] (dimensions in mm). Source: Trindade et al. [13].

The decision to simulate standard beams based on characterization tests was made considering the abundance of available data in the literature. The availability of such extensive data enables a comprehensive analysis, particularly in terms of static considerations, providing a greater level of accuracy in the conducted analyses. This is especially important when evaluating properties that have the potential to influence model behaviors.

2.3 Post-cracking parameters

The behavior in tension of SFRC is expressed in terms of residual flexural tensile strength $f_{R,j}$ (j = 1, 2, 3, 4) corresponding to $CMOD_j$ ($CMOD_1$= 0.5 mm, $CMOD_2$= 1.5 mm, $CMOD_3$= 1.5 mm and $CMOD_4$= 3.5 mm), as presented in Equation 1:

$$f_{R,j} = \frac{3 \cdot F_j \cdot l}{2 \cdot b \cdot {h_{sp}}^2} \quad (1)$$

where F_j = measured point load at mid-span of the test specimen (MPa); l = span length (m); b = width (m); and h_{sp} = distance between the tip of the notch and the top of the beam in the mid-span section (m).

The limit of proportionality f_L can be determined by applying Equation 2:

$$f_L = \frac{3 \cdot F_{LOP} \cdot l}{2 \cdot b \cdot {h_{sp}}^2} \quad (2)$$

where F_{LOP} = highest measured load between $0 \leq CMOD \leq 0.05$ mm (MPa).

3 ANALYTICAL PROCEDURE

The sectional analysis method was used to predict the bending behavior of SFRC test standard beams, whose dimensions and test methodology are standardized by EN 14651 [14]. This method allows to simulate of the nonlinear response and describes the cracking and post-cracking behavior of sections built with different materials. As a result, it is possible to obtain the load-CMOD diagrams of the critical sections of the elements under study.

In this perspective, an analytical model was used to obtain the flexural behavior of SFRC. The algorithm was based on a procedure similar to that described by [3], [4], [11], given its simplicity and accuracy. Fundamental principles and assumptions of the model are presented below.

3.1 Basic assumptions

The following assumptions were made:

1. Sections remain plane after loading or imposed strains (hypothesis of Navier-Bernoulli);
2. Strain compatibility: perfect bond between concrete and fibers;
3. Shear distortion and stresses are negligible and, for this reason, were not considered (hypothesis of Euler-Bernoulli);
4. Internal forces are applied on the symmetrical axis of the section.

3.2 Section idealization

A schematic representation of the element cross-section, the linear strain, and stress distribution is represented in Figure 3. In the analysis, it was also assumed that the stresses located in the upper part of the section refer to compressive stresses, while the stresses located in the lower part refer to tensile stresses.

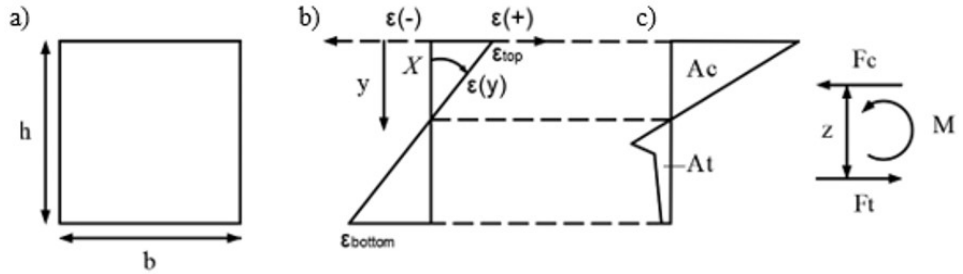

Figure 3. Schematic representation of a) the cross-section, b) the distribution of strains, c) the distribution of stresses. Source: Adapted from Galeote et al. [11].

The constitutive models used for simulating the stress-strain response of the studied sections were the RILEM [17], Model Code [18] and Código Estructural [6]. In the subsequent discussion, these models will be referred to as RILEM, MC2010 and CE2021, respectively. The response of the SFRC under compression, as well as the response up to the peak load in the tensioned region of the section, assumes the linear elastic behavior before reaching the cracking load of the constitutive models. After the peak load, the non-linear relation of the constitutive models is employed to simulate the post-cracking behavior. Table 1 presents an overview of the constitutive models proposed in the aforementioned documents, along with the parameters defining each model.

Table 1. Constitutive models to simulate the stress-strain behavior of SFRC. Source: Adapted from Álvarez et al. [4].

Diagram	Parameters	Reference
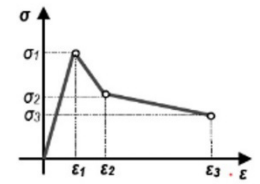	$\sigma_1 = 0.7 \cdot fctm_{fl} \cdot (1.6 - d)$	RILEM [17]
	$\sigma_2 = 0.45 \cdot K_h \cdot f_{R,1}$	
	$\sigma_3 = 0.37 \cdot K_h \cdot f_{R,4}$	
	$\varepsilon_1 = \sigma_1 \,/\, E_{HRF}$	
	$\varepsilon_2 = \varepsilon_2 + 0.1‰$	
	$\varepsilon_3 = \varepsilon_u = 25‰$	
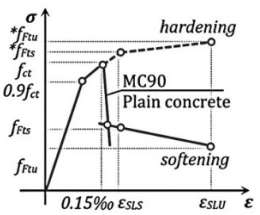	$f_{Fts} = 0.45 \times f_{R1}$	MC2010 [18]
	$f_{Ftu} = k \times [f_{Fts} - (w_u/CMOD_3) \times (f_{Fts} - 0.5 \times f_{R3} + 0.2 \times f_{R1})]$	
	$\varepsilon_{SLS} = CMOD_1/l_{cs}$	
	$\varepsilon_{SLU} = \frac{w_u}{l_{cs}} = \min\left(\varepsilon_{Fu} = \frac{2.5}{l_{cs}} = \frac{2.5}{y}\right)$	
	$\varepsilon_{Fu} = (20‰\ softening;\ 10‰\ hardening)$	
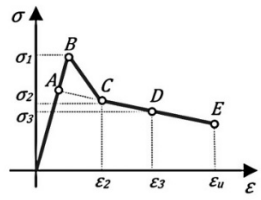	$\sigma_1 = f_{ct,d} = 0.6 \times f_{ct,fl,d}$	CE2021 [6]
	$\sigma_2 = f_{ctR1,d} = 0.45 \times f_{R,1,d}$	
	$\sigma_3 = f_{ctR3,d} = k_1 \times (0.5 \times f_{R,3,d} - 0.2 \times f_{R,1,d})$	
	$\varepsilon_2 = 0.1 + 1000 \times f_{ct,d}/E_{c,0}$	
	$\varepsilon_3 = 2.5/l_{cs} (lcs: characteristic\ lenght)$	
	$\varepsilon_u = (20‰\ bending;\ 10‰\ pure\ tension)$	

where $fctm_{fl}$ = average flexural tensile strength of concrete (MPa), d = effective depth of the section (m), K_h = the size factor; $CMOD_i$ = crack mouth opening displacement, i = 1, 2, 3 or 4, of which $CMOD_1$ = 0.5 mm, $CMOD_2$ = 1.5 mm, $CMOD_3$ = 2.5 mm, $CMOD_4$ = 3.5 mm; $f_{R,i}$ = residual flexural tensile strength for a $CMOD_i$ (MPa); $E_{HRF} = E_{c,0}$ = modulus of elasticity of SFRC (MPa); $k = k_1$ = coefficient for the type of stresses in the cross-section; w_u = ultimate crack width (mm); l_{cs} = characteristic length (m); y = height of the neutral axis (m); $f_{ct,fl,d}$ = design value of the flexural tensile strength of concrete (MPa) and $f_{ct,d}$ = design tensile strength of concrete (MPa).

The crack width, necessary for the elaboration of the load-CMOD graph, was obtained according to Equation 3 proposed by MC2010.

$$w = l_{cs} \times \varepsilon_{bottom} \tag{3}$$

where ε_{bottom} = strain at the bottom layer of the section (‰).

The characteristic length is an indicator of the crack spacing used in calculations whose value is influenced by several factors such as type and volume of fibers, matrix strength, cross-section geometry, load level (service, ultimate), etc [11]. Studies in the literature reveal that there is not a clear consensus to specify l_{cs} and researchers use different criteria to determine its value [19].

In this paper, the recommendation of MC2010 was considered ($l_{cs} = h_{sp}$), where h_{sp} is the distance between the top of the notch and the top of the specimen. According to the characterization test indicated to obtain the parameters of MC2010 (EN 14651 [14]), h_{sp} should be 125 mm ± 1 mm for specimens with 150 mm height.

3.3 Equilibrium and compatibility

The equilibrium between sectional stresses and external forces is obtained by imposing the Equation 4 and Equation 5. Moreover, Hypothesis of Navier and the perfect bond (Equation 6) between the different materials forming the section are considered.

$$N = F_t \cdot A_t = F_c \cdot A_c \tag{4}$$

where N = external axial force; M = external bending moment, F_c = compressive stress, F_t = tensile stress, A_c = compressed area, A_t = tensile area.

$$M = F_t \cdot A_t \cdot z = F_c \cdot A_c \cdot z \tag{5}$$

where z = lever arm between the forces.

$$\varepsilon_{(y)} = \varepsilon_{top} - y \cdot \chi \tag{6}$$

where $\varepsilon_{(y)}$ = strain along the section ε_{top} = strain in the upper layer, y = height of the concerned layer and χ = curvature.

3.4 Strategy adopted to solve the sectional problem

The calculation procedure that allowed the analysis of cross sections of SFRC test standard beams is shown in the flowchart of Figure 4. The method begins assuming an initial strain at the bottom fiber and calculates the strains at the cross-section by an iterative process checking whether the equilibrium conditions are satisfied. When a result is achieved, the strain at the bottom increases and the iterative process starts over.

Results from experimental campaigns, carried out by third parties, were used for validation of the load-CMOD curve analytically obtained. Thus, to obtain more precision in the comparative analysis, the calculation of the percentage error was performed, according to Equation 7, to evaluate which models are closer or farther from the experimental data. Moreover, the error value was also used to evaluate the ability of some predetermined parameters to influence the bending behavior of SFRC test standard beams.

$$\%\, error = \frac{F_{an} - F_{exp}}{F_{exp}} \cdot 100 \tag{7}$$

where F_{an} = strength calculated with the analytical model and F_{exp} = strength from experimental tests taken from the literature.

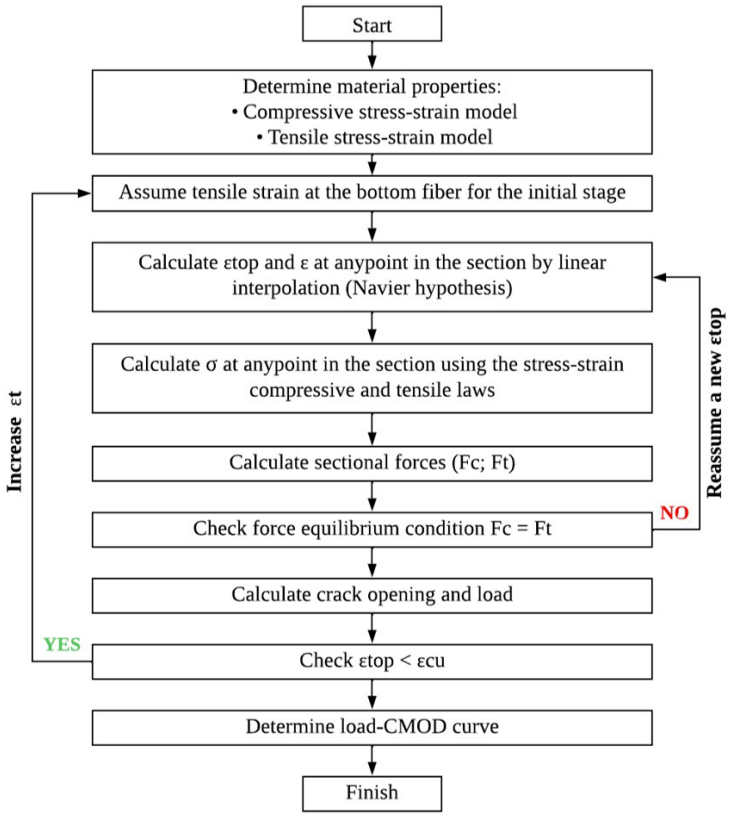

Figure 4. Flow chart of the analytical cross-sectional model. Source: Adapted from Galeote et al. [11].

4 COMPARISON OF PREDICTIONS AND EXPERIMENTAL RESULTS

Figure 5 and Figure 6 show load-crack opening graphs obtained experimentally and analytically for concretes reinforced with different volumes of steel fibers. In these graphs, the results of the experimental tests extracted from the literature [13], [16] were plotted, as well as the curves obtained analytically through the multi-linear diagrams proposed by the RILEM, MC2010 and CE2021 standards.

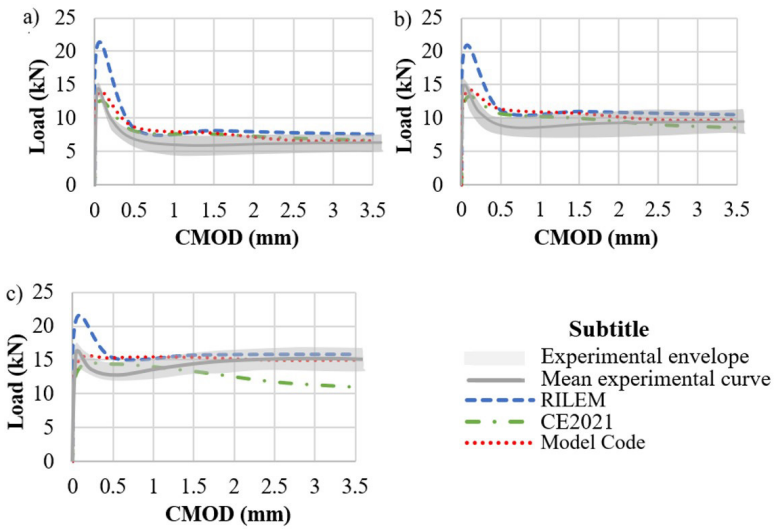

Figure 5. Load-CMOD curves obtained using volumes of steel fibers in the following variations: (a) 0.19%, (b) 0.32% and (c) 0.45%.

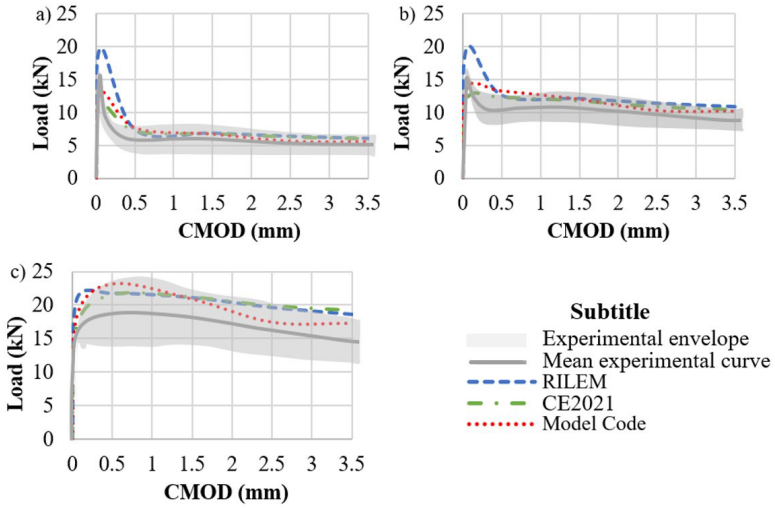

Figure 6. Load-CMOD curves obtained using volumes of steel fibers in the following variations: (a) 0.19%, (b) 0.38% e (c) 0.58%.

It can be seen from Figure 5 and Figure 6 that the model proposed by RILEM predicts significantly higher cracking load values compared to the other models represented, revealing an overestimation of the structural response of the element. On the other hand, CE2021 has lower cracking load values than the others, resulting in a more conservative behavior in the failure phase. The model proposed by MC2010, however, presented results for the peak load that were closest to those found by the average experimental curves.

The equation that best predicts the resisted load for a crack opening of 0.5 mm (F_1) was proposed by CE2021. On the other hand, it can be seen that the model that worst predicts this drop in resistance capacity is MC2010. The RILEM model showed intermediate results. Although the CE2021 and RILEM models are closer to the average curve, they still insecurely predict the moment right after the SFRC cracking.

Concerning residual loads, the MC2010 equation presents predictions that best fit the experimental response. The RILEM model exhibited values that, although within the experimental envelope, are higher than the average values. In relation to the CE2021 model, it was not possible to identify a pattern in the behavior of residual loads, since they differed in the works used as a reference.

In Figure 6c, there is a load-CMOD curve indicative of deflection-hardening behavior. For this case, it was clear that in terms of peak load, the CE2021 model presented the best predictions. On the other hand, the MC2010 model exhibited values of residual loads lower than the value of the other models, thus showing a more assertive prediction of behavior for this region of the diagram. It should be noted that, despite the proximity of some models to the experimental average, all equations showed behaviors that tend to be on the side of insecurity.

5 EVALUATION OF THE INFLUENCE OF DIFFERENT PARAMETERS ON THE FORECASTS OF THE CONSTITUTIVE MODELS

In order to better understand the differences between the experimental campaigns collected in the literature and the analytical models, a statistical analysis was performed. To this end, residual strength values of 528 standard steel fiber reinforced concrete beams with variable concrete and fiber characteristics were taken from the literature [15]. Then the collected strength values were transformed into load values (according to Equation 1 and Equation 2), and the experimental results obtained by other works [13], [16] were added to this data set (Figure 5 and Figure 6, respectively).

Subsequently, the extensive range of test results of standard SFRC beams obtained was divided according to the average compressive strength of the concrete matrix, the fiber volume, the fiber aspect ratio and the ultimate tensile strength of the fibers. Each of the mentioned parameters was divided into two groups, so that they would have a similar amount of data, with the exception of the compressive strength of the matrix that was separated into low or high-performance concrete. Table 2 presents how the data segmentation was performed.

Table 2. Database classification.

Parameter	Group 1	Group 2
Mean compressive strength, MPa	≤50	> 50
Volume fraction of fibers, %	≤ 0.5	> 0.5
Fiber aspect ratio	≤ 60	> 60
Fiber tensile strength, MPa	≤ 1345	> 1345

Such partition is intended to provide an organized discussion of the influence of these parameters in the prediction of resisted loads by the SFRC based on a detailed analysis of the errors obtained between the analytical models studied and the experimental data of each group. Therefore, for each of the classifications, the error was calculated in percentage terms for the five main points resulting from the three-point bending tests (F_{LOP}, F_1, F_2, F_3 e F_4).

Table 3 presents the averages and standard deviations (in parentheses next to the average) of the calculated percentage errors for such points of the graph of all the groups of parameters under study (Table 2).

In addition to Table 3, ANOVA and Tukey's test were performed to assess whether the difference in the error results obtained was statistically significant between the models and in relation to itself with the change of group. For this purpose, box-plot graphs were plotted for the five main points resulting from the three-point bending tests, presenting in each graph the percentage error values obtained by each model, considering the division of Table 2 for the entire database studied. It is worth mentioning that results that differed drastically from all the others were discarded for the analysis of the average error previously presented, and were represented in the graphs as outliers to avoid distortions in the results. The box-plot graphs for each parameter studied, that is, the average compressive strength of the matrix, fiber volume, form factor and ultimate tensile strength of the fibers, are illustrated in Figure 7-10, respectively.

Table 3. Averages and standard deviation of the calculated percentage errors of each constitutive model for the main points of the load-CMOD graph, considering the different classifications.

Identification		Flop	F1	F2	F3	F4
≤50 MPa	RILEM	0.40 (0.14)	0.20 (0.05)	0.16 (0.08)	0.18 (0.1)	0.24 (0.1)
	MC2010	-0.01 (0.14)	0.17 (0.04)	0.13 (0.15)	0.15 (0.25)	0.21 (0.29)
	CE2021	0.09 (0.14)	0.25 (0.04)	0.15 (0.07)	0.07 (0.04)	0.18 (0.08)
>50 MPa	RILEM	0.56 (0.15)	0.19 (0.04)	0.1 (0.06)	0.1 (0.06)	0.18 (0.07)
	MC2010	0.04 (0.14)	0.15 (0.03)	0.02 (0.10)	-0.03 (0.16)	0.02 (0.20)
	CE2021	0.08 (0.16)	0.22 (0.04)	0.09 (0.06)	0.03 (0.03)	0.13 (0.06)
≤0.5%	RILEM	0.54 (0.16)	0.23 (0.04)	0.12 (0.08)	0.12 (0.08)	0.20 (0.12)
	CE2021	-0.02 (0.13)	0.18 (0.03)	0.05 (0.14)	-0.01 (0.19)	0.04 (0.24)
	MC2010	0.03 (0.15)	0.26 (0.04)	0.11 (0.08)	0.04 (0.04)	0.14 (0.08)
>0.5%	RILEM	0.47 (0.15)	0.17 (0.03)	0.11 (0.05)	0.13 (0.07)	0.20 (0.08)
	CE2021	0.05 (0.11)	0.13 (0.02)	0.05 (0.10)	0.04 (0.18)	0.10 (0.24)
	MC2010	0.12 (0.15)	0.21 (0.03)	0.10 (0.05)	0.04 (0.03)	0.15 (0.07)
≤60	RILEM	0.47 (0.14)	0.20 (0.04)	0.13 (0.06)	0.14 (0.08)	0.23 (0.09)
	CE2021	-0.04 (0.09)	0.16 (0.03)	0.09 (0.13)	0.06 (0.18)	0.16 (0.27)
	MC2010	0.02 (0.13)	0.25 (0.04)	0.13 (0.06)	0.06 (0.04)	0.17 (0.08)
>60	RILEM	0.55 (0.19)	0.19 (0.05)	0.1 (0.07)	0.11 (0.08)	0.17 (0.08)
	CE2021	0.06 (0.13)	0.15 (0.04)	0.02 (0.12)	-0.02 (0.19)	0.03 (0.23)
	MC2010	0.10 (0.14)	0.22 (0.04)	0.09 (0.07)	0.03 (0.05)	0.12 (0.07)
≤1345 MPa	RILEM	0.49 (0.18)	0.21 (0.04)	0.16 (0.08)	0.16 (0.09)	0.23 (0.09)
	CE2021	-0.04 (0.11)	0.17 (0.03)	0.11 (0.14)	0.10 (0.23)	0.15 (0.26)
	MC2010	0.02 (0.11)	0.26 (0.04)	0.15 (0.07)	0.06 (0.04)	0.17 (0.08)
>1345 MPa	RILEM	0.55 (0.16)	0.19 (0.03)	0.08 (0.05)	0.08 (0.05)	0.15 (0.06)
	CE2021	0.04 (0.13)	0.14 (0.03)	-0.02 (0.09)	-0.1 (0.14)	-0.06 (0.18)
	MC2010	0.08 (0.17)	0.21 (0.03)	0.07 (0.05)	0.02 (0.03)	0.11 (0.07)

5.1 Mean compressive strength of the matrix

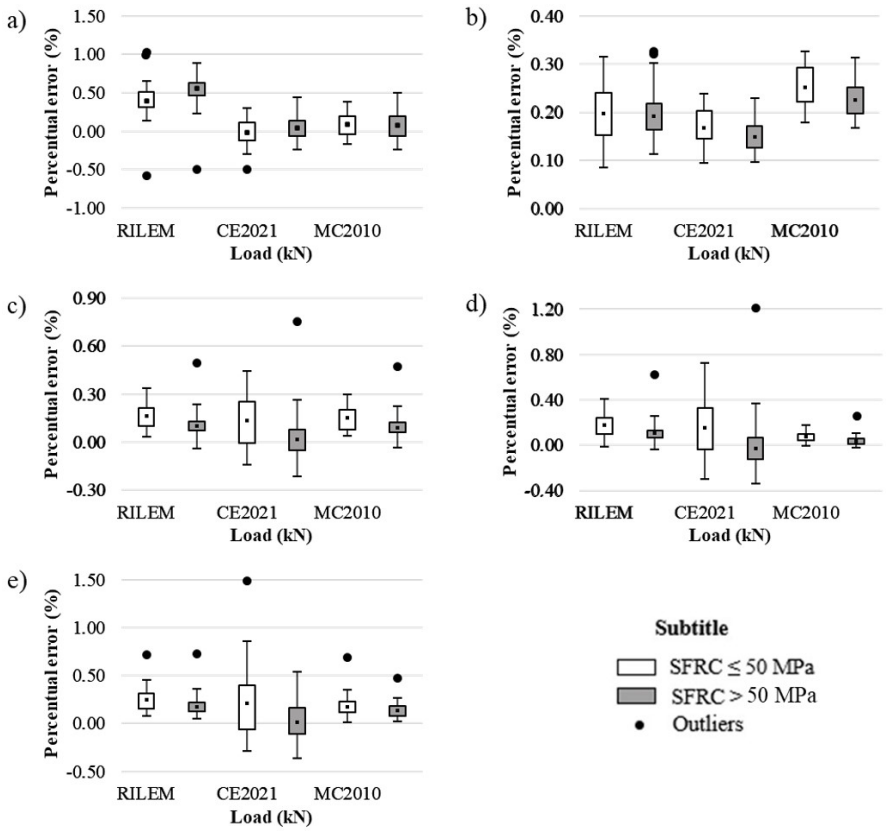

Figure 7. Box-plot of the percentage errors, considering different mean compressive strength of the matrix, for the load values corresponding to the following CMODs: 0.05 mm (a), 0.5 mm (b), 1.5 mm (c), 2.5 mm (d), 3.5 mm (e).

It was verified by the ANOVA test that all load values, illustrated in Figure 7, show a difference from a statistical point of view in the prediction made by each of the models under study (p-value ≤ 7.395E-06 in all ANOVA comparisons). That is, for the division performed, based on the average compressive strength of the matrix (SRFC ≤ 50 MPa and SFRC > 50 MPa), the constitutive laws presented estimates of load values for each crack opening, which differ considerably among one another.

With regard to peak load (Figure 7a), according to the Tukey test, the RILEM model was different from the other models studied and from itself when separated into different groups of compressive matrix strength (p-value ≤ 0.002731). The other models were not significantly different in the group divisions. Analyzing Table 3, the RILEM model presented average results of smaller errors for concretes with strengths lower than 50 MPa. On the other hand, the MC2010 and CE2021 models showed a similar average error value and standard deviation for both groups, showing that their predictions are not significantly influenced by this parameter.

Regarding the residual loads (Figure 7b to Figure 7e), according to Tukey's test, only the CE2021 model was statistically different for the group division performed (p-value ≤ 2.255 E-4). This constitutive law also showed the greatest differences in error values in relation to the other two models studied. It was verified in Table 3 that all models show better results for residual loads for concrete with strengths greater than 50 MPa in terms of both average error and standard deviation.

5.2 Fiber volume

ANOVA indicated that all points, except F_4 (p-value = 0.133), had statistically different error values among the models. It is worth noting that the loads F_2 e F_3 presented p-values (0.01164 and 0.002532, respectively) which, despite still indicating statistical difference, were quite high compared to those obtained for F_1 and F_{LOP} (p-value ≤ 8.287E-47), thus demonstrating a low divergence in the responses of the models for the loads F_2 and F_3 when faced with variations in the volume of fibers (see Figure 8).

Regarding the load F_L (Figure 8a), it is observed that all concrete volumes were better predicted by models CE2021 and MC2010. Despite this, it is noted that the prediction of the RILEM model indicates slight signs of improvement with increasing fiber volume, contrary to the other two models that have lower error values for lower fiber volumes. The results of the Tukey test confirm that for the cracking load, there is a statistical difference between the errors calculated for the models CE2021 and MC2010 in relation to those of the RILEM (p-value = 0). Despite the difference between the models, the Tukey test did not verify the influence of the fiber volume variation in the prediction of the cracking load by the models.

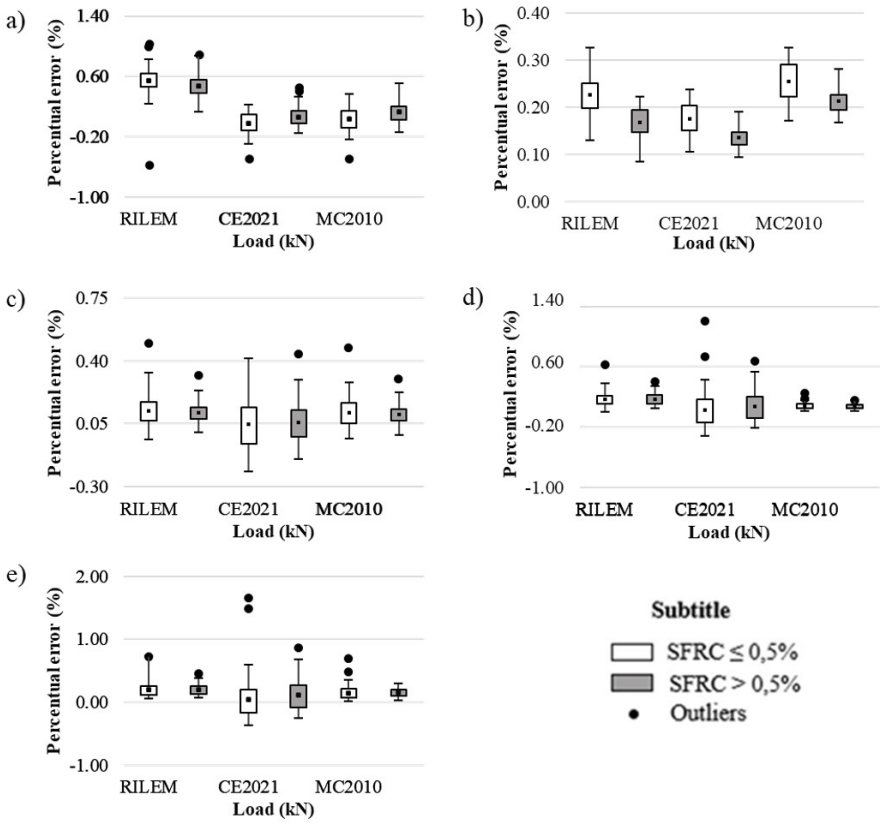

Figure 8. Box-plot of the percentage errors, considering different fiber volume, for the load values corresponding to the following CMODs: 0.05 mm (a), 0.5 mm (b), 1.5 mm (c), 2.5 mm (d), 3.5 mm (e).

When analyzing Table 3, it appears that the residual loads did not show uniformity in the results obtained. For F_1 and F_2, concretes with volume above 0.5% presented greater precision, while for F_3 and F_4, the error values were very similar. In the Tukey test, the loads F_2 and F_4 did not present statistical differences between the models. The load F_3 showed a small difference only between the CE2021 and the RILEM models (p-value $<$ 0.033). The largest discrepancies were verified for the load F_1, where the RILEM model differs from the others and in relation to itself in the division of groups. The other models also differ in the division of groups for the load F_1 (p-value $\leq$ 9.542E-05 in the Tukey test). Such a discussion can also be seen in Figure 8b to Figure 8e.

Regarding ANOVA, the constitutive models showed statistically different predictions for all load values, with the lowest p-value found for loads F_4 and F_2 (0.001322 and 0.0003918, respectively). This indicates that there is a difference in the predictions of the models, as well as a possible influence of the fiber aspect ratio on the force resisted by the SFRC for each crack opening, as can be seen in Figure 9.

It is worth noting that all the models under analysis were more accurate in predicting the cracking loads of fiber-reinforced concrete with a fiber aspect ratio of less than 60, as can be seen in Figure 9a. In addition to this, the Tukey test showed that for the peak load, the RILEM model differs from the other models studied, but it does not differ statistically in relation to itself regarding the variation of the fiber aspect ratio. The other models, MC2010 and CE2021, showed a slight statistical difference with the division of the groups according to the fiber aspect ratio (p-value $\leq$ 0.04489).

5.3 Fiber aspect ratio

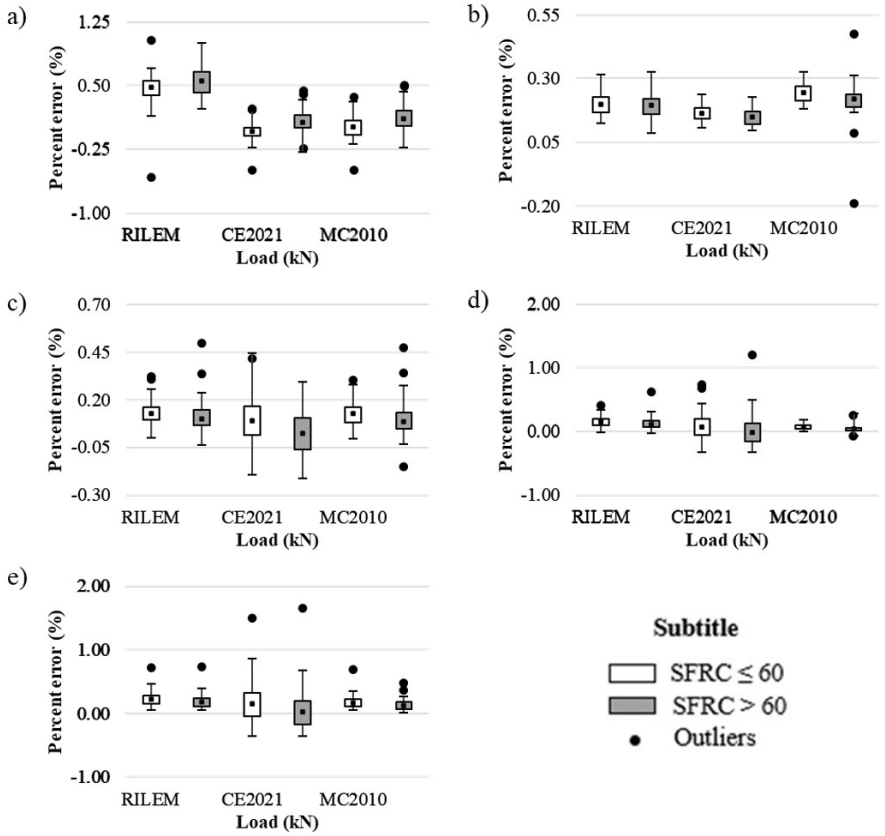

Fig. 9. Box-plot of the percentage errors, considering different fiber aspect ratio, for the load values corresponding to the following CMODs: 0.05 mm (a), 0.5 mm (b), 1.5 mm (c), 2.5 mm (d), 3.5 mm (e).

On the other hand, according to Table 3, residual loads were better predicted in 100% of cases for fiber-reinforced concrete with a fiber aspect ratio greater than 60 (Figure 9b to Figure 9e). Furthermore, in the Tukey test, all residual loads showed statistical differences between the CE2021 and RILEM models (p-value ≤ 0.02591). In the analysis of the Tukey test for the load F_1, all the models showed statistical differences among themselves, but not in relation to themselves. The only point where any model was influenced by the fiber aspect ratio was for the load F_4, where, according to Tukey's test, the CE2021 model shows a difference with the division of the group (p-value = 0.03092).

5.4 Ultimate fiber tensile strength

ANOVA indicates that for all load values studied, there is a statistical difference between the predictions made by each of the constitutive laws under study (p-value ≤ 1.45E-09), as illustrated in Figure 10.

Regarding the cracking load (Figure 10a), the RILEM model was statistically different from both the MC2010 and the CE2021 (p-value = 0) in the Tukey test, although it did not show great divergence in the predictions with the ultimate fiber tensile strength variation. The other models were also not influenced by the variation of the parameter studied for the peak load. In addition, it was possible to verify in Table 3 that the fibers of lower strength showed greater precision in the prediction of the cracking load, a fact that can also be observed in Figure 10a.

Residual loads were significantly affected by the variation of the tensile strength of the fibers (Figure 10b to Figure 10e). Proof of this is that at all residual loads, the CE2021 model presented differences in the predictions with the change in the ultimate fiber tensile strength (p-value ≤ 0.01578) according to the Tukey test. For the load F_1, in addition to CE2010, MC2010 also presented divergences in the results with the division of groups. For the load F_2, all models were shown to be influenced by the change in fiber strength. Regarding the predictions of the models as a whole, without taking into account the division of groups according to the ultimate fiber tensile strength, the Tukey test indicated statistical differences in general (p-value ≤ 0.04991).

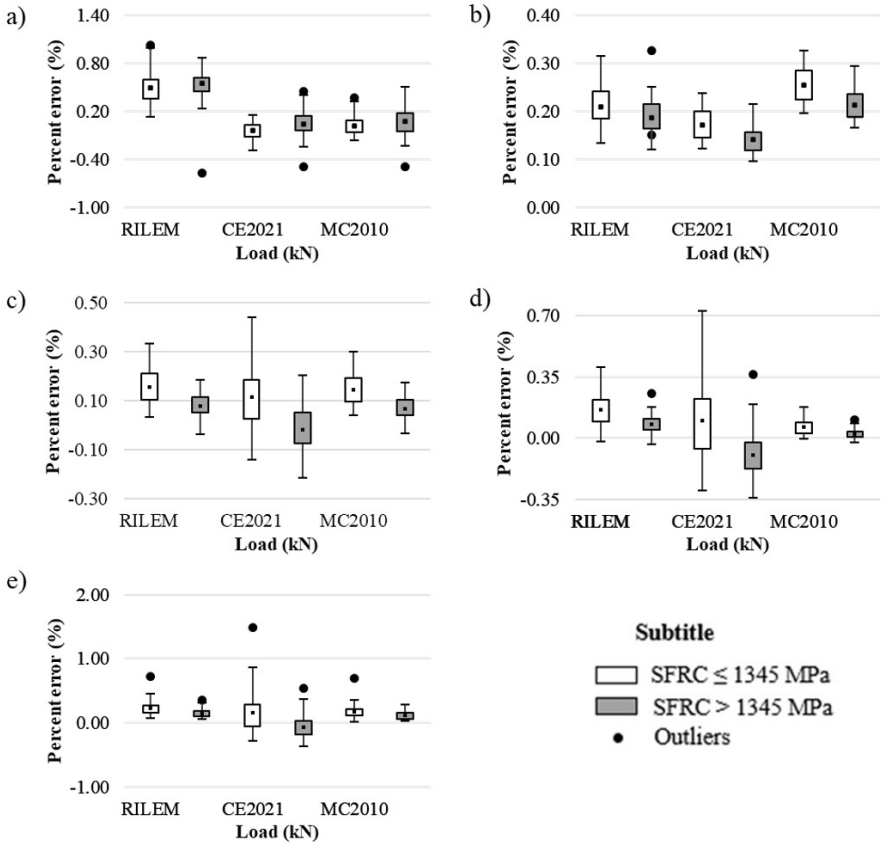

Figure 10. Box-plot of the percentage errors, considering different tensile strengths of the fibers, for the load values corresponding to the following CMODs: 0.05 mm (a), 0.5 mm (b), 1.5 mm (c), 2.5 mm (d), 3.5 mm (e).

It is also worth noting that for residual loads, the models showed a lower error and standard deviation values for fiber-reinforced concrete with strength greater than 1345 MPa in all cases. Therefore, it is understood that the models studied are better at predicting the residual loads of fiber-reinforced concrete with higher tensile strengths. However, with regard to cracking load, fibers with lower strengths showed superior performance in the prediction provided by the constitutive laws.

6 CONCLUSIONS

Based on the results and discussions presented, the following conclusions can be highlighted regarding the comparison between the constitutive laws:

- For the cracking load (F_L), RILEM predicted overestimated values, CE2021 presented a more conservative behavior and MC2010 was the model that came closest to the experimental average curves;
- The equation that best predicted the resisted load for a crack opening of 0.5 mm (F_1) was the one proposed by CE2021, with MC2010 being the one that worst predicted this drop in resistance capacity, while RILEM showed intermediate results;
- Regarding the residual loads (F_2, F_3 and F_4), the MC2010 equation presents the predictions that best fit the experimental response. RILEM exhibited values higher than the average values. For CE2021, it was not possible to identify a pattern of behavior from the analyzed data;
- For SFRC with a deflection-hardening curve, the peak load was best estimated by CE2021, while MC2010 exhibited the best approximations regarding residual loads. However, for this type of curve, all equations showed behaviors that tended towards insecurity.

Regarding the parameters capable of influencing the SFRC tensile response, the following conclusions are evident:

- The average compressive strength of the matrix has a relevant influence on the result when the RILEM model is used to predict the cracking load and when CE2021 is used to predict the residual loads. The other models were barely influenced by the variation of this parameter. There was a subtle improvement in the ability to predict residual loads for high strength concretes and cracking load when simulated concretes with fck ≤ 50 MPa;

- In relation to fiber volume, for residual loads, with the exception of F_1, the models did not show relevant differences in the predictions performed, thus proving little influenced by this parameter. The cracking load, on the other hand, showed significant differences in the predicted results between the models. However, the difference in relation to the division of groups according to fiber volume was not significant. Thus, it is understood that the volume of fibers is capable of influencing the prediction of the point right after the cracking load (F_1), with the other loads barely being influenced by its variation;
- Only the MC2010 and CE2021 models were influenced by the form factor in relation to the cracking load, but the difference was not relevant. With regard to residual loads, no considerable influence of the models' predictions was observed with the variation of the form factor. Although there is no significant impact on the response, the cracking load is better estimated for form factors < 60, while residual loads present better results for form factors > 60;
- The ultimate tensile strength of the fibers proved to be a parameter capable of significantly influencing the results of load resisted by the SFRC, since different values of error were found for the same model, only varying the tensile strength. The CE2021 model can be highlighted, which was the most susceptible to variation in this parameter.

Based on the conducted analyses, it can generally be concluded that the studied equations have the potential to predict the post-cracking behavior of SFRC. However, it is crucial to emphasize the necessity of evaluating the representativeness of the characterization tests in relation to full-scale structural elements. This is due to the significant disparities in structural response and fiber orientation between small beams and larger-sized elements. Consequently, it is imperative to investigate the representativeness of the conclusions presented about the models or the influence of the properties on full-scale structural elements. This would provide a more comprehensive understanding of the post-cracking behavior of SFRC and enhance the reliability of predictions in practical engineering scenarios.

ACKNOWLEDGEMENTS

The first author thanks Coordenação de Aperfeiçoamento de Pessoal de Nível Superior – Brasil (CAPES) – Finance Code 001 for financial support. This work also has been supported by the research project CNPq/MCTI/FNDCT Nº 18/2021 422189/2021-9; RTI2018-099091-B-C22. All authors thank the PPGEC (Postgraduate Program in Civil Engineering) and CESEC (Centre for Civil Engineering Studies) at UFPR for their institutional support.

REFERENCES

[1] T. Ikumi, E. Galeote, P. Pujadas, A. de la Fuente, and R. D. López-Carreño, "Neural network-aided prediction of post-cracking tensile strength of fibre-reinforced concrete," *Comput. Struc.*, vol. 256, pp. 106640, 2021.

[2] T. E. T. Buttignol, J. Fernandes, T. N. Bittencourt, and J. L. A. O. Sousa, "Design of reinforced concrete beams with steel fibers in the ultimate limit state," *Rev. IBRACON Estrut. Mater.*, vol. 11, pp. 997–1024, 2018.

[3] A. de la Fuente, A. Aguado, and C. Molins, "Numerical model for the non linear analysis of precast and sequentially constructed sections," *Hormig. Acero.*, vol. 57, no. 247, pp. 69–87, 2008.

[4] A. B. Álvarez, P. P. Álvarez, A. de la Fuente Antequera, and A. A. de Cea, "Análisis comparativo de los modelos constitutivos del hormigón reforzado con fibras," *Hormig. Acero.*, vol. 61, no. 256, pp. 83–101, 2010.

[5] Associação Brasileira de Normas Técnicas, *Projeto de Estruturas de Concreto Reforçado com Fibras – Procedimento*, NBR 16935, 2021.

[6] España, "Código Estructural: Anejo 7: Recomendaciones para la utilización de hormigón con fibras, CE," *Bol. Of. Estado*, 2021.

[7] Comisión Permanente Del Hormigón, *Instrucción del Hormigón Estructural*, EHE-08, 2008.

[8] Deutscher Ausschuss für Stahlbeton, *Richtlinie Stahlfaserbeton*, DAfStb, 2010.

[9] Deutscher Beton-Und Bautechnik-Verein E.V, *Guide to Good Practice Steel Fibre Concrete*. Berlin: DBV, 2001.

[10] A. Blanco, P. Pujadas, A. de la Fuente, S. Cavalaro, and A. Aguado, "Application of constitutive models in European codes to RC–FRC," *Constr. Build. Mater.*, vol. 40, pp. 246–259, 2013.

[11] E. Galeote, A. Blanco, and A. de la Fuente, "Design-oriented approach to determine FRC constitutive law parameters considering the size effect," *Compos. Struct.*, vol. 239, pp. 112036, 2020.

[12] V. M. C. F. Cunha, J. A. O. Barros, and J. M. Sena-Cruz, "A finite element model with discrete embedded elements for fibre reinforced composites," *Comput. Struc.*, vol. 94, pp. 22–33, 2012.

[13] Y. T. Trindade, L. A. Bitencourt Jr., R. Monte, A. D. de Figueiredo, and O. L. Manzoli, "Design of SFRC members aided by a multiscale model: Part I–Predicting the post-cracking parameters," *Compos. Struct.*, vol. 241, pp. 112078, 2020.

[14] European Committee for Standardization, *Test Method for Metallic Fiber-Reinforced Concrete – Measuring the Flexural Tensile Strength (Limit of Proporcionality - LOP), Residual*, EN 14651, 2007.

[15] G. Tiberti, F. Germano, A. Mudadu, and G. A. Plizzari, "An overview of the flexural post-cracking behavior of steel fiber reinforced concrete," *Struct. Concr.*, vol. 19, no. 3, pp. 695–718, 2018.

[16] R. P. Salvador, “Análise comparativa de métodos de ensaio para caracterização do comportamento mecânico de concreto reforçado com fibras,” M.S. thesis, Polytech. Sch., Univ. São Paulo, São Paulo, 2013.

[17] RILEM, "RILEM TC 162-TDF: test and design methods for steel fibre reinforced concrete sigma-epsilon-design method – final recommendation," *Mater. Struct.*, vol. 36, pp. 560–567, 2003.

[18] International Federation for Structural Concrete, *fib Bulletin 65: Model Code for Concrete Structures, Final Draft: 5.6 Fibres/Fibre Reinforced Concrete*, vol. 1, 2010.

[19] R. Montaignac, B. Massicotte, and J. P. Charron, "Design of SFRC structural elements: flexural behaviour prediction," *Mater. Struct.*, vol. 45, no. 4, pp. 623–636, 2012.

Author contributions: FF: conceptualization, data curation, formal analysis, methodology, writing; HMK: formal analysis, writing—review and editing; RP: conceptualization, methodology, supervision, reviewing.

Editors: Osvaldo Manzoli, Guilherme Aris Parsekian.